

Topology and Spectrum in Measurement-Induced Phase Transitions

Hisanori Oshima,^{1,2} Ken Mochizuki,^{1,2} Ryusuke Hamazaki,^{2,3} and Yohei Fuji¹

¹*Department of Applied Physics, University of Tokyo, Tokyo 113-8656, Japan*

²*Nonequilibrium Quantum Statistical Mechanics RIKEN Hakubi Research Team, RIKEN CPR, Wako, Saitama 351-0198, Japan*

³*RIKEN iTHEMS, Wako, Saitama 351-0198, Japan*

(Dated: December 17, 2024)

Competition among repetitive measurements of noncommuting observables and unitary dynamics can give rise to a rich variety of entanglement phases. We here characterize topological phases in monitored quantum systems by their spectrum and many-body topological invariants. We analyze (1+1)-dimensional monitored circuits for Majorana fermions, which have topological and trivial area-law entangled phases and a critical phase with sub-volume-law entanglement, through the Lyapunov spectrum. We uncover the presence (absence) of edge-localized zero modes inside the bulk gap in the topological (trivial) area-law phase and a bulk gapless spectrum in the critical phase. Furthermore, by suitably exploiting the fermion parity with twisted measurement outcomes at the boundary, we construct a topological invariant that sharply distinguishes the two area-law phases and dynamically characterizes the critical phase. Our work thus paves the way to extend the bulk-edge correspondence for topological phases from equilibrium to monitored quantum dynamics.

Introduction.— Topology is undoubtedly one of the most essential concepts in understanding stable phases of matter [1]. For ground states of local Hamiltonians with a finite excitation gap, states belonging to distinct topological phases cannot be smoothly deformed to each other without closing the gap, owing to discrete characters of their topological invariants [2]. In particular, for symmetry-protected topological phases [3–8], nontrivial topology of the bulk leads to gapless boundary states robust against any symmetry-preserving perturbations. This phenomenon, known as the bulk-edge correspondence, has remarkable consequences in physical properties of the topological phases and has been intensively studied in the past few decades [9–13].

Despite notable successes in equilibrium systems, topology in out-of-equilibrium systems caused by external environment has yet to be fully understood. In particular, it is still elusive how the topology plays a role in monitored quantum systems, which gather a recent extensive interest as they host novel non-equilibrium phases concerning, e.g., entanglement [14–25]. Indeed, repetitive measurements stabilizing distinct topological phases can lead to phase transitions between different entanglement phases, which can be probed by topological entanglement entropy or purification dynamics [26–42] (see also [43–45]). However, intrinsic spatiotemporal randomness caused by the probabilistic nature of measurement outcomes makes it difficult to generalize more standard notions of topological phases, such as bulk topological invariants and gapless edge modes, to monitored systems.

In this Letter, we discover gapless edge modes and a bulk topological invariant that characterize measurement-induced phase transitions of monitored Majorana circuits and discuss their bulk-edge correspondence. Introducing effective Hamiltonians obtained through the Lyapunov analysis, we reveal the presence (absence) of edge-localized zero modes inside the bulk

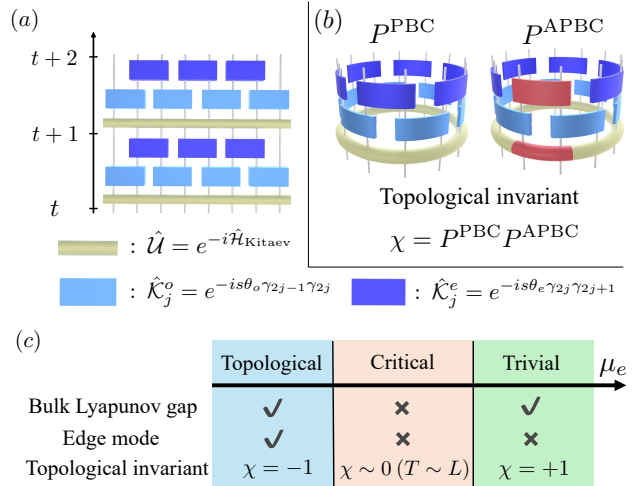


FIG. 1. (a) Monitored quantum circuit for Majorana fermions. In each time step, after unitary time evolution generated by $\hat{\mathcal{H}}_{\text{Kitaev}}$ in Eq. (1), we weakly measure the Majoranas in the brickwork manner with Kraus operators (2). (b) Bulk topological invariant χ for the monitored system, obtained from the fermion parities $P^{\text{PBC/APBC}}$ for circuits under PBC/APBC. The APBC involves the boundary measurement operators with twisted outcomes for the PBC. (c) The measurement-induced phases characterized by the Lyapunov gap, existence of the edge mode, and our topological invariant. The topological (trivial) gapped phase exhibits the presence (absence) of edge mode and $\chi = -1$ ($\chi = +1$). The gapless critical phase is characterized by the dynamical behavior of χ .

gap in the topological (trivial) area-law phase. We also construct a bulk topological invariant based on the fermion parity, extending the method in equilibrium systems to the monitored setting; this is accomplished by introducing a unique boundary condition with twisted measurement outcomes. The invariant sharply distinguishes these gapped area-law phases, featuring the bulk-

edge correspondence. Moreover, we show that the critical entanglement phase corresponds to a gapless phase concerning the Lyapunov spectrum. While the bulk-edge correspondence is obscured in this phase, we demonstrate that the topological invariant can still *dynamically* characterize the two gapped and gapless phases. Our result is summarized in Fig. 1.

Model and Lyapunov analysis.— We consider a (1+1)-dimensional quantum circuit acting on $2L$ Majorana fermions [see Fig. 1(a)], which consists of repeated applications of three elementary steps: (i) unitary time evolution \hat{U} , (ii) measurements of all Majorana pairs on odd bonds, and (iii) measurements of all Majorana pairs on even bonds. Applying these three operations on a state $|\psi_t\rangle$, we obtain a state $|\psi_{t+1}\rangle$ updated by a single time step. To be more precise, the unitary evolution is given by the Kitaev chain Hamiltonian, $\hat{U} = e^{-i\hat{\mathcal{H}}_{\text{Kitaev}}}$, with

$$\hat{\mathcal{H}}_{\text{Kitaev}} = iJ \sum_{\ell=1}^{2L-1} \gamma_\ell \gamma_{\ell+1} + iJ' \gamma_{2L} \gamma_1, \quad (1)$$

where γ_ℓ are Majorana fermions obeying $\{\gamma_\ell, \gamma_{\ell'}\} = 2\delta_{\ell\ell'}$ and J, J' are real constants. The measurements of Majorana pairs on odd/even bonds with an outcome $s = \pm 1$ are described by the Kraus operators,

$$\hat{\mathcal{K}}_j^o(s) = \frac{e^{-is\theta_o \gamma_{2j-1} \gamma_{2j}}}{\sqrt{2 \cosh(2\theta_o)}}, \quad \hat{\mathcal{K}}_j^e(s) = \frac{e^{-is\theta_e \gamma_{2j} \gamma_{2j+1}}}{\sqrt{2 \cosh(2\theta_e)}}. \quad (2)$$

which are weak measurements of the strength $\theta_{e/o} = \tanh^{-1}(\mu_{e/o})$. We set $\mu_e = 1 - \mu_o$ hereafter. Given a (unnormalized) state $|\psi\rangle$, each outcome s is obtained with the Born probability, $p_j^{e/o}(s) = \langle\psi|(\hat{\mathcal{K}}_j^{e/o}(s))^\dagger \hat{\mathcal{K}}_j^{e/o}(s)|\psi\rangle / \langle\psi|\psi\rangle$. In the following, we use three boundary conditions: open (OBC), periodic (PBC), and antiperiodic (APBC). For the unitary evolution \hat{U} , the boundary condition is simply specified by J' : $J' = 0, J$, and $-J$ for the OBC, PBC, and APBC, respectively. For the measurements, the OBC means that we discard $\hat{\mathcal{K}}_L^e(s)$ from the circuit, while we need a careful definition of the APBC, as we will explain later.

At the time $t = T$, an initial state $|\psi_0\rangle$ is evolved by the Kraus operator labeled by a sequence of outcomes $\mathbf{s} = \{\mathbf{s}_1, \dots, \mathbf{s}_T\}$ with $\mathbf{s}_t = \{s_{1,t}, \dots, s_{2L,t}\}$,

$$\hat{\mathcal{K}}_T(\mathbf{s}) = \prod_{t=1}^T \left(\left(\prod_j \hat{\mathcal{K}}_j^e(s_{2j,t}) \right) \left(\prod_j \hat{\mathcal{K}}_j^o(s_{2j-1,t}) \right) \hat{U} \right). \quad (3)$$

Since both unitary evolution and measurements are bilinear in Majorana fermions, this circuit maps a fermionic Gaussian state to another Gaussian state [46–52]. A fermionic Gaussian state is completely characterized by the Majorana covariance matrix Γ_t whose element reads $(\Gamma_t)_{\ell\ell'} = (i/2) \langle \psi_t | [\gamma_\ell, \gamma_{\ell'}] |\psi_t\rangle / \langle \psi_t | \psi_t \rangle$. Time evolution of the (unnormalized) Gaussian state is encoded

in the transformation of the Majorana fermions, $\vec{\gamma} \rightarrow \hat{\mathcal{K}}_T(\mathbf{s})^\dagger \vec{\gamma} (\hat{\mathcal{K}}_T(\mathbf{s})^\dagger)^{-1} = K_T(\mathbf{s}) \vec{\gamma}$, where

$$K_T(\mathbf{s}) = \prod_{t=1}^T \left(e^{-i\tilde{\Theta}^e(\mathbf{s}_t)} e^{-i\tilde{\Theta}^o(\mathbf{s}_t)} e^{\tilde{H}_{\text{Kitaev}}} \right). \quad (4)$$

Here, $\tilde{H}_{\text{Kitaev}}$ and $\tilde{\Theta}^{e/o}(\mathbf{s}_t)$ are real antisymmetric matrices defined through $\hat{\mathcal{H}}_{\text{Kitaev}} = i\vec{\gamma}^\top \tilde{H}_{\text{Kitaev}} \vec{\gamma}/4$ and $\prod_j \hat{\mathcal{K}}_j^{e/o}(s_{2j/2j-1,t}) \propto \exp(i\vec{\gamma}^\top \tilde{\Theta}^{e/o}(\mathbf{s}_t) \vec{\gamma}/4)$ with $\vec{\gamma} = (\gamma_1, \dots, \gamma_{2L})^\top$ (see Supplemental Material [53]).

Since this circuit $K_T(\mathbf{s})$ is a product of random matrices, we can perform the Lyapunov analysis [54–60]. Provided that the Oseledec theorem [61–63] holds, the Lyapunov spectrum z_ℓ does not depend on the sequence of outcomes \mathbf{s} . It is also related to the energy spectrum of the effective Hamiltonian,

$$H_{\text{eff},T}(\mathbf{s}) = -\frac{i}{2T} \ln[K_T(\mathbf{s}) K_T(\mathbf{s})^\dagger], \quad (5)$$

and the corresponding many-body Hamiltonian $\hat{\mathcal{H}}_{\text{eff},T}(\mathbf{s}) = -i\vec{\gamma}^\top H_{\text{eff},T}(\mathbf{s}) \vec{\gamma}/4$. Since $H_{\text{eff},T}(\mathbf{s})$ is real antisymmetric, its eigenvalues $iz_{\ell,T}(\mathbf{s}) \in i\mathbb{R}$ come in pairs, $z_{2j-1,T}(\mathbf{s}) = -z_{2j,T}(\mathbf{s})$. This defines the single-particle energy spectrum $z_{\ell,T}(\mathbf{s})$, which in the asymptotic limit coincides with the Lyapunov spectrum: $z_\ell = \lim_{T \rightarrow \infty} z_{\ell,T}(\mathbf{s})$. We below arrange them as $0 \leq z_1 = -z_2 \leq \dots \leq z_{2L-1} = -z_{2L}$. We can also compute the corresponding Lyapunov vectors $\vec{w}_{\ell,T}(\mathbf{s})$. Written in the matrix form $\tilde{O}_T(\mathbf{s}) = (\vec{w}_{1,T}(\mathbf{s}), \dots, \vec{w}_{2L,T}(\mathbf{s}))$, they give in the asymptotic limit an orthogonal matrix that brings $H_{\text{eff},T}(\mathbf{s})$ into the standard form,

$$\lim_{T \rightarrow \infty} \tilde{O}_T(\mathbf{s})^\top H_{\text{eff},T}(\mathbf{s}) \tilde{O}_T(\mathbf{s}) = \bigoplus_{j=1}^L \begin{pmatrix} 0 & z_{2j-1} \\ -z_{2j-1} & 0 \end{pmatrix}. \quad (6)$$

In practice, we construct $\tilde{O}_T(\mathbf{s})$ through computing Lyapunov vectors corresponding to the non-negative Lyapunov spectrum based on the complex fermion representation, which is equivalent to the Majorana representation [53]. In the following, we only look at a single trajectory specified by a typical sequence of \mathbf{s} and consider a temporal average of quantities in the long-time limit unless otherwise mentioned [53].

Lyapunov edge modes in measurement-only circuits.—

We first perform the Lyapunov analysis for the measurement-only circuit ($J = J' = 0$). In this case, a direct transition at $\mu_e \simeq 0.5$ occurs from a topological to a trivial area-law phase, as numerically checked by the topological entanglement entropy and bipartite mutual information [53], as done in [34, 41, 42].

Remarkably, we reveal that the topologically nontrivial area-law phase is characterized by Majorana zero modes for the Lyapunov spectrum. In Fig. 2(a), we plot the non-negative single-particle Lyapunov spectrum z_k against μ_e

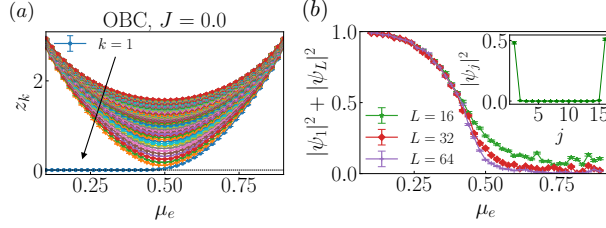


FIG. 2. (a) Non-negative single-particle Lyapunov spectra for $L = 64$ and (b) sum of squared amplitudes of the spinor wavefunction corresponding to the lowest energy z_1 at the edges for the measurement-only circuit with the OBC. We find that the topologically non-trivial phase hosts a spatially localized Majorana edge mode with the zero Lyapunov exponent. The inset in (b) shows the spatial distribution of squared amplitudes of the spinor wavefunction at $t = 2L$ averaged over 1000 different trajectories for $L = 16$ and $\mu_e = 0.1$.

for the measurement-only circuit under the OBC for $L = 64$. Importantly, z_1 takes a finite value for $\mu_e > 0.5$, while it vanishes for $\mu_e \leq 0.5$. Vanishing of z_1 under the OBC in the topological area-law phase implies the many-body Lyapunov gap closing for $\hat{\mathcal{H}}_{\text{eff},T}(\mathbf{s})$, which is reminiscent of Majorana zero modes for the static Kitaev chain [64].

We next show that the above zero mode is a spatially localized edge mode by analyzing the spinor wavefunction $\vec{\psi}_T(\mathbf{s})$ [65] with its element $(\vec{\psi}_T(\mathbf{s}))_j = \sqrt{\sum_{a=1,2} \sum_{b=2j-1,2j} ((\vec{w}_{a,T}(\mathbf{s}))_b^2)/2}$ corresponding to the lowest energy $z_{1,T}(\mathbf{s}) \simeq z_1$. In Fig. 2(b), We plot the long-time average of the sum of the squared amplitudes for $\vec{\psi}_T(\mathbf{s})$ at both edges, $|(\vec{\psi}_T(\mathbf{s}))_1|^2 + |(\vec{\psi}_T(\mathbf{s}))_L|^2$, against μ_e . Deep inside the topological phase ($\mu_e \ll 0.5$), it takes a value close to 1 regardless of the system size, signaling localization of the zero mode near the edges. In contrast, it decreases toward a value $2/L$ in the trivial phase, indicating that the Majorana mode delocalizes over the whole lattice on average. The localization of the zero modes in the topological phase is much more visible if we directly look at the spatial profile of the $|(\vec{\psi}_T(\mathbf{s}))_j|^2$. The inset of Fig. 2(b) shows (trajectory-averaged) values of $|(\vec{\psi}_T(\mathbf{s}))_j|^2$ for $L = 16$ and $\mu_e = 0.1$. These results indicate that the Lyapunov spectrum clearly reveals edge-localized Majorana zero modes in the topological area-law phase.

Topological invariant and bulk-edge correspondence.—

We now introduce a bulk topological invariant and relate it with the presence (absence) of the Lyapunov edge modes in the topological (trivial) area-law phase. Since the circuit $\hat{\mathcal{K}}_T(\mathbf{s})$ conserves the fermion parity $\hat{P} = \prod_{j=1}^L i\gamma_{2j-1}\gamma_{2j}$, the eigenstates of the effective Hamiltonian $\hat{\mathcal{H}}_{\text{eff},T}(\mathbf{s})$ have definite parities ± 1 unless they are degenerate. We then define the topological invariant as a difference between the fermion parities computed for the ground state under the PBC and that under the APBC. While this is analogous to the procedure

for static Kitaev chains [64, 66, 67], a special care is required to determine the APBC because the trajectories depend on measurement outcomes. Namely, the APBC is here defined *with respect to the PBC*; we generate a circuit under the PBC with a sequence of measurement outcomes \mathbf{s} . Then the circuit under the APBC is defined by flipping the outcomes $s_{2L,t}$ only for the boundary Majorana pairs, $\hat{\mathcal{K}}_L^e(s_{2L,t}) \rightarrow \hat{\mathcal{K}}_L^e(-s_{2L,t})$, with $\hat{\mathcal{U}}$ under the APBC. Using $\hat{\mathcal{H}}_{\text{eff},T}^{\text{PBC/APBC}}(\mathbf{s})$ defined through the above prescription, we introduce the topological invariant as the product of their ground states' parities. Since the parity can be computed as the sign of the Pfaffian of the single-particle Hamiltonian for noninteracting systems, which is known as Kitaev's formula [64], the topological invariant for monitored Majorana circuits is given by

$$Q_T(\mathbf{s}) = \text{sgn}(\text{Pf}[H_{\text{eff},T}^{\text{PBC}}(\mathbf{s})]\text{Pf}[H_{\text{eff},T}^{\text{APBC}}(\mathbf{s})]). \quad (7)$$

However, the explicit form of $H_{\text{eff},T}(\mathbf{s})$ is numerically intractable for large T . Thus, we instead compute $\chi_T(\mathbf{s})$ defined by

$$\chi_T(\mathbf{s}) = P_T^{\text{PBC}}(\mathbf{s})P_T^{\text{APBC}}(\mathbf{s}), \quad (8)$$

$$P_T^{\text{PBC/APBC}}(\mathbf{s}) = \det[\tilde{O}_T^{\text{PBC/APBC}}(\mathbf{s})]. \quad (9)$$

Since $\chi_T(\mathbf{s})$ approximates and converges to $Q_T(\mathbf{s})$ for $T \rightarrow \infty$, we will also call $\chi_T(\mathbf{s})$ as the topological invariant. We note that $\tilde{O}_T^{\text{PBC/APBC}}(\mathbf{s})$ is not an orthogonal matrix for general T .

In Fig. 3, we show the lowest single-particle Lyapunov spectrum z_1 for the measurement-only circuit under the (a) PBC and (b) APBC. It takes a finite value for both cases, implying a finite bulk Lyapunov gap, within each area-law phase. As shown in Fig. 3(c), the topological invariant $\chi_T(\mathbf{s})$ clearly separates the topological and trivial area-law phases. Note that these results are qualitatively independent of the measurement outcomes \mathbf{s} . In fact, $P_T^{\text{PBC}}(\mathbf{s}) = 1$ is satisfied in the whole parameter region, since the gap does not close at the transition $\mu_e = 0.5$ for PBC due to finite-size splitting $z_1 \sim 1/L$. On the other hand, $P_T^{\text{APBC}}(\mathbf{s})$ abruptly changes from -1 to $+1$ across the transition point for APBC, implying an exact gap closing near $\mu_e = 0.5$. This results in the observed transition in $\chi_T(\mathbf{s})$. The behaviors of the bulk Lyapunov gap resemble those of the bulk energy gap ΔE of the static translation-invariant Kitaev chain [64]; in that case, $\Delta E = 0$ for PBC and $\Delta E \sim 1/L$ for APBC at the transition, across which the Pfaffian invariant changes its sign.

The edge-localized zero mode under the OBC in Fig. 2 and the topological invariant in Fig. 3 indicate that the bulk-edge correspondence applies even to nonequilibrium phases under temporally random measurements, if the bulk gap is open. Such an exploration based on topology in random dynamics is accomplished by the Lyapunov analysis and the appropriate definition of the topological

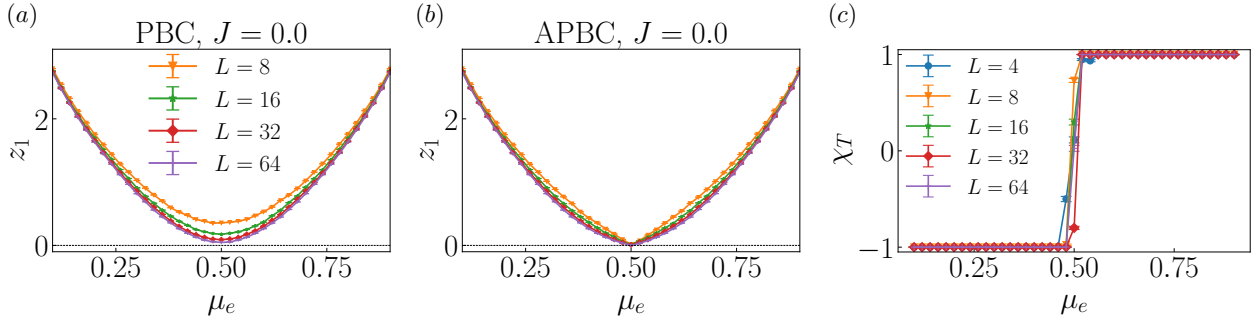


FIG. 3. (a,b) Lowest non-negative single-particle Lyapunov spectrum for the measurement-only circuit with (a) PBC and (b) APBC. They are gapped except for $\mu_e \simeq 0.5$, where z_1 behaves as $\sim 1/L$ for PBC and the exact gap closing is anticipated for APBC. (c) Topological invariant after a sufficiently long time, which sharply characterizes topological and trivial phases.

invariant via effective Hamiltonians. Note that a naive quantity $P_T^{\text{PBC}}(\mathbf{s})P_T^{\text{APBC}}(\mathbf{s}')$ with $\mathbf{s} \neq \mathbf{s}'$ does not provide a good topological invariant in general. Rather, focusing on the trajectory under the APBC dependent on the trajectory under PBC makes their fermion parities meaningful to define the invariant under random measurements.

Gapless critical phase with additional unitary.— We now study the monitored circuit with unitary dynamics by the Kitaev Hamiltonian $\hat{\mathcal{H}}_{\text{Kitaev}}$ and discuss how the Lyapunov spectrum and the topological invariant behave. Reference [51] considered a continuous-time version of our model to find three different entanglement phases as μ_e increases. Specifically, the unitary part leads to a critical phase whose entanglement scales as $S \sim (\ln L)^2$ between the topological and trivial area-law phases (see also [37–42, 68–71]). In our circuit model, we numerically find three entanglement phases separated by two transition points $\mu_e \simeq 0.4$ and $\simeq 0.6$ for $J = 0.5$, using the topological entanglement entropy and bipartite mutual information [53].

To discuss the topology of the three phases, we first investigate the Lyapunov spectrum in the circuit with OBC, finding that the critical phase corresponds to a gapless phase without Majorana zero modes. Figure 4(a) shows the μ_e dependence of the non-negative single-particle Lyapunov spectrum. As observed in the measurement-only case, the lowest mode z_1 become gapless (gapped) in the topological (trivial) phase. In the critical phase for $0.4 \lesssim \mu_e \lesssim 0.6$, not only the lowest mode z_1 but also higher modes $z_{k(\neq 1)}$ appear to become gapless, implying the closing of the bulk Lyapunov gap. Interestingly, the L -dependence of z_1 seems different between the topological area-law phase and the critical phase; z_1 exponentially decays in L in the topological area-law phase ($\mu_e \lesssim 0.4$), while it appears to decay in $1/L$ for our available system sizes in the critical phase ($0.4 \lesssim \mu_e \lesssim 0.6$) [53].

The above observation of the bulk spectrum is also confirmed from the lowest spectrum z_1 under the PBC

and APBC. Indeed, as shown in Fig. 4(b,c), z_1 goes to zero for $0.4 \lesssim \mu_e \lesssim 0.6$, whereas the bulk gap is open for other μ_e . While the scaling form of z_1 right at the transitions $\mu_e \simeq 0.4$ and 0.6 is close to $1/L$, it appears to decay faster than $1/L$ inside the critical phase (except the APBC circuit at $\mu_e = 0.5$, where exact gap closing is anticipated nearby) [53].

The above results for the spectral gaps indicate that the bulk-edge correspondence is obscured for the gapless phase if we consider $\chi_\infty \equiv \lim_{T \rightarrow \infty} \chi_T(\mathbf{s})$ for finite L , which is confirmed to be convergent irrespective of \mathbf{s} . That is, since z_1 can only be exactly zero near $\mu_e = 0.5$ for APBC, the asymptotic topological invariant can switch the sign only at this point for finite system sizes. Indeed, we have numerically observed that χ_T flows towards -1 for $\mu_e < 0.5$ and $+1$ for $\mu_e > 0.5$ as T increases [53]. In contrast, as discussed above, the Majorana zero mode seems absent even for $0.4 \lesssim \mu_e < 0.5$. Therefore, while the critical phase is unstable in static Majorana chains and is thus unique to monitored Majorana chains, the bulk-edge correspondence is obscured since it corresponds to the gapless phase. This is reminiscent of the fact that topological phase is usually well defined in the gapped phase in static systems.

Remarkably, however, we find that the topological invariant *dynamically* characterizes the different phases, including the critical gapless phase. Specifically, we consider the sample-averaged invariant, χ_T , for the timescale $T = \mathcal{O}(L)$. Figure 4(d) shows $\chi_{T=L}$ for different system sizes, from which we find three crossings with $\mu_e \simeq 0.4, 0.5$, and 0.6 . The locations of the first and last crossings coincide well to the transitions between the area-law gapped phases and critical gapless phase. Notably, this characterization is attributed to the divergent relaxation time of the invariant in the gapless phase. If we denote the timescale as τ_{relax} , it is at least longer than $\sim z_1^{-1}$, which increases faster than L inside the gapless phase. Therefore, $\chi_{T=L}$ will not converge and almost stay zero for the gapless phase. This is contrasted to the gapped phases with $z_1 = \mathcal{O}(L^0)$, where χ_T rapidly con-

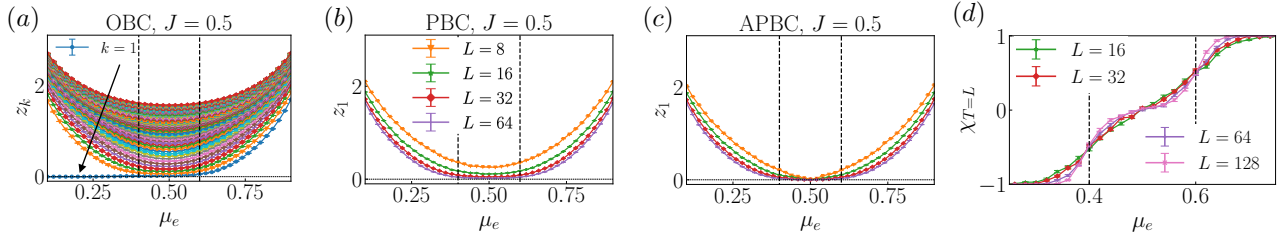


FIG. 4. (a) Non-negative single-particle Lyapunov spectrum for the monitored circuit with $J = 0.5$ under the OBC for $L = 64$. (b,c) Lowest non-negative spectrum z_1 under the (b) PBC and (c) APBC. (d) Topological invariant at $t = L$ averaged over 1000 different trajectories. The Lyapunov spectrum and topological invariant distinguish the topological area-law, critical gapless, and trivial area-law phases at $\mu_e \simeq 0.4$ and 0.6 , as indicated by the dashed vertical lines.

verge to ± 1 for $T = \mathcal{O}(L)$. Note that the crossing point at $\mu_e \simeq 0.5$ is different from the boundaries of the three phases. The above argument indicates that this crossing is a finite-size artifact, and $\chi_{T=L}$ will flatly become zero in the entire critical phase for $L \rightarrow \infty$.

Summary and outlook.— We have shown that monitored Majorana circuits in the gapped phases exhibit the bulk-edge correspondence through investigating the Lyapunov spectrum, gapless edge modes, and topological invariants based on the fermion parity. To define the topological invariant, we have used a unique methodology where the trajectory under APBC is defined with respect to that under PBC, according to twisted measurement outcomes at the boundary. We have also shown that the critical phase corresponds to the gapless phase in terms of the Lyapunov spectrum and is dynamically characterized by the topological invariant in a timescale $t = \mathcal{O}(L)$.

Our study opens the way to explore topological features in monitored systems through the Lyapunov analysis. An important future direction is to examine many-body systems, where our topological invariant based on the twisted measurement outcomes readily applies. For example, it is intriguing to analyze monitored circuits with $Z_2 \times Z_2$ symmetry, for which measurements can stabilize an area-law phase with a symmetry-protected topological order of the cluster state [26, 32, 38]. Such a topological area-law phase will be characterized by (nearly) four-fold degenerate Lyapunov spectrum under the OBC from gapless edge modes and a topological invariant measuring the change of one Z_2 charge by twisting boundary measurement outcomes for another Z_2 symmetry.

Note added.— While this work was in its final stage, we learned about a recent paper which investigates a similar issue [72].

Acknowledgements— We thank Xhek Turkeshi, Henning Schomerus, Alessandro Romito, Amos Chan, Keiji Saito, Ken Shiozaki, and Takahiro Morimoto for valuable discussions and comments. We thank Zhenyu Xiao and Kohei Kawabata for coordinating the submission of this work and Ref. [72]. H.O. is supported by RIKEN Junior Research Associate Program. K. M. and R.H.

are supported by JST ERATO Grant Number JPMJER2302, Japan. K.M. is supported by JSPS KAKENHI Grant No. JP23K13037. R.H. is supported by JSPS KAKENHI Grant No. JP24K16982. Y.F. is supported by JSPS KAKENHI Grants No. JP20K14402 and No. JP24K06897. Part of the computation has been performed using the facilities of the Supercomputer Center, the Institute for Solid State Physics, the University of Tokyo.

-
- [1] X.-G. Wen, Colloquium: Zoo of quantum-topological phases of matter, *Rev. Mod. Phys.* **89**, 041004 (2017).
 - [2] X. Chen, Z.-C. Gu, and X.-G. Wen, Local unitary transformation, long-range quantum entanglement, wave function renormalization, and topological order, *Phys. Rev. B* **82**, 155138 (2010).
 - [3] Z.-C. Gu and X.-G. Wen, Tensor-entanglement-filtering renormalization approach and symmetry-protected topological order, *Phys. Rev. B* **80**, 155131 (2009).
 - [4] F. Pollmann, A. M. Turner, E. Berg, and M. Oshikawa, Entanglement spectrum of a topological phase in one dimension, *Phys. Rev. B* **81**, 064439 (2010).
 - [5] X. Chen, Z.-C. Gu, and X.-G. Wen, Classification of gapped symmetric phases in one-dimensional spin systems, *Phys. Rev. B* **83**, 035107 (2011).
 - [6] L. Fidkowski and A. Kitaev, Topological phases of fermions in one dimension, *Phys. Rev. B* **83**, 075103 (2011).
 - [7] Y.-M. Lu and A. Vishwanath, Theory and classification of interacting integer topological phases in two dimensions: A Chern-Simons approach, *Phys. Rev. B* **86**, 125119 (2012).
 - [8] X. Chen, Z.-C. Gu, Z.-X. Liu, and X.-G. Wen, Symmetry protected topological orders and the group cohomology of their symmetry group, *Phys. Rev. B* **87**, 155114 (2013).
 - [9] M. Z. Hasan and C. L. Kane, Colloquium: Topological insulators, *Rev. Mod. Phys.* **82**, 3045 (2010).
 - [10] X.-L. Qi and S.-C. Zhang, Topological insulators and superconductors, *Rev. Mod. Phys.* **83**, 1057 (2011).
 - [11] T. Senthil, Symmetry-Protected Topological Phases of Quantum Matter, *Ann. Rev. Condens. Matter Phys.* **6**, 299 (2015).
 - [12] E. Witten, Fermion path integrals and topological

- phases, *Rev. Mod. Phys.* **88**, 035001 (2016).
- [13] C.-K. Chiu, J. C. Y. Teo, A. P. Schnyder, and S. Ryu, Classification of topological quantum matter with symmetries, *Rev. Mod. Phys.* **88**, 035005 (2016).
- [14] Y. Li, X. Chen, and M. P. A. Fisher, Quantum Zeno effect and the many-body entanglement transition, *Phys. Rev. B* **98**, 205136 (2018).
- [15] B. Skinner, J. Ruhman, and A. Nahum, Measurement-Induced Phase Transitions in the Dynamics of Entanglement, *Phys. Rev. X* **9**, 031009 (2019).
- [16] A. Chan, R. M. Nandkishore, M. Pretko, and G. Smith, Unitary-projective entanglement dynamics, *Phys. Rev. B* **99**, 224307 (2019).
- [17] M. Szyniszewski, A. Romito, and H. Schomerus, Entanglement transition from variable-strength weak measurements, *Phys. Rev. B* **100**, 064204 (2019).
- [18] Y. Li, X. Chen, and M. P. A. Fisher, Measurement-driven entanglement transition in hybrid quantum circuits, *Phys. Rev. B* **100**, 134306 (2019).
- [19] C.-M. Jian, Y.-Z. You, R. Vasseur, and A. W. W. Ludwig, Measurement-induced criticality in random quantum circuits, *Phys. Rev. B* **101**, 104302 (2020).
- [20] Y. Bao, S. Choi, and E. Altman, Theory of the phase transition in random unitary circuits with measurements, *Phys. Rev. B* **101**, 104301 (2020).
- [21] S. Choi, Y. Bao, X.-L. Qi, and E. Altman, Quantum Error Correction in Scrambling Dynamics and Measurement-Induced Phase Transition, *Phys. Rev. Lett.* **125**, 030505 (2020).
- [22] M. J. Gullans and D. A. Huse, Dynamical Purification Phase Transition Induced by Quantum Measurements, *Phys. Rev. X* **10**, 041020 (2020).
- [23] M. J. Gullans and D. A. Huse, Scalable Probes of Measurement-Induced Criticality, *Phys. Rev. Lett.* **125**, 070606 (2020).
- [24] A. C. Potter and R. Vasseur, Entanglement Dynamics in Hybrid Quantum Circuits, in *Entanglement in Spin Chains: From Theory to Quantum* edited by A. Bayat, S. Bose, and H. Johannesson (Springer International Publishing, Cham, 2022) pp. 211–249.
- [25] M. P. Fisher, V. Khemani, A. Nahum, and S. Vijay, Random Quantum Circuits, *Ann. Rev. Condens. Matter Phys.* **14**, 335 (2023).
- [26] A. Lavasani, Y. Alavirad, and M. Barkeshli, Measurement-induced topological entanglement transitions in symmetric random quantum circuits, *Nat. Phys.* **17**, 342 (2021).
- [27] A. Lavasani, Y. Alavirad, and M. Barkeshli, Topological Order and Criticality in (2 + 1)D Monitored Random Quantum Circuits, *Phys. Rev. Lett.* **127**, 235701 (2021).
- [28] K. Klocke and M. Buchhold, Topological order and entanglement dynamics in the measurement-only XZZX quantum code, *Phys. Rev. B* **106**, 104307 (2022).
- [29] A. Lavasani, Z.-X. Luo, and S. Vijay, Monitored quantum dynamics and the Kitaev spin liquid, *Phys. Rev. B* **108**, 115135 (2023).
- [30] A. Sriram, T. Rakovszky, V. Khemani, and M. Ippoliti, Topology, criticality, and dynamically generated qubits in a stochastic measurement-only Kitaev model, *Phys. Rev. B* **108**, 094304 (2023).
- [31] G.-Y. Zhu, N. Tantivasadakarn, and S. Trebst, Structured volume-law entanglement in an interacting, monitored Majorana spin liquid (2023), arXiv:2303.17627 [quant-ph].
- [32] R. Morral-Yepes, F. Pollmann, and I. Lovas, Detecting and stabilizing measurement-induced symmetry-protected topological phases in generalized cluster models, *Phys. Rev. B* **108**, 224304 (2023).
- [33] Y. Kuno and I. Ichinose, Production of lattice gauge Higgs topological states in a measurement-only quantum circuit, *Phys. Rev. B* **107**, 224305 (2023).
- [34] R. Nehra, A. Romito, and D. Meidan, Controlling measurement induced phase transitions with tunable detector coupling (2024), arXiv:2404.07918 [quant-ph].
- [35] C. Kelson-Packer and A. Miyake, Phase transitions in (2 + 1)D subsystem-symmetric monitored quantum circuits (2024), arXiv:2407.18340 [quant-ph].
- [36] K. Klocke, D. Simm, G.-Y. Zhu, S. Trebst, and M. Buchhold, Entanglement dynamics in monitored Kitaev circuits: loop models, symmetry classification, and quantum Lifshitz scaling (2024), arXiv:2409.02171 [quant-ph].
- [37] A. Nahum and B. Skinner, Entanglement and dynamics of diffusion-annihilation processes with Majorana defects, *Phys. Rev. Res.* **2**, 023288 (2020).
- [38] Y. Bao, S. Choi, and E. Altman, Symmetry enriched phases of quantum circuits, *Ann. Phys.* **435**, 168618 (2021), special issue on Philip W. Anderson.
- [39] C.-M. Jian, H. Shapourian, B. Bauer, and A. W. W. Ludwig, Measurement-induced entanglement transitions in quantum circuits of non-interacting fermions: Born-rule versus forced measurements (2023), arXiv:2302.09094 [cond-mat.stat-mech].
- [40] K. Klocke and M. Buchhold, Majorana Loop Models for Measurement-Only Quantum Circuits, *Phys. Rev. X* **13**, 041028 (2023).
- [41] G. Kells, D. Meidan, and A. Romito, Topological transitions in weakly monitored free fermions, *SciPost Phys.* **14**, 031 (2023).
- [42] H. Pan, H. Shapourian, and C.-M. Jian, Topological Modes in Monitored Quantum Dynamics (2024), TechnoRxiv:2411.04191, [quant-ph].
- [43] N. Lang and H. P. Büchler, Entanglement transition in the projective transverse field Ising model, *Phys. Rev. B* **102**, 094204 (2020).
- [44] S. Sang and T. H. Hsieh, Measurement-protected quantum phases, *Phys. Rev. Res.* **3**, 023200 (2021).
- [45] M. Ippoliti, M. J. Gullans, S. Gopalakrishnan, D. A. Huse, and V. Khemani, Entanglement Phase Transitions in Measurement-Only Dynamics, *Phys. Rev. X* **11**, 011030 (2021).
- [46] S. Bravyi, Lagrangian representation for fermionic linear optics, *Quantum Inf. Comput.* **5**, 216–238 (2005).
- [47] X. Turkeshi, A. Biella, R. Fazio, M. Dalmonte, and M. Schiró, Measurement-induced entanglement transitions in the quantum Ising chain: From infinite to zero clicks, *Phys. Rev. B* **103**, 224210 (2021).
- [48] J. Surace and L. Tagliacozzo, Fermionic Gaussian states: an introduction to numerical approaches, *SciPost Phys. Lect. Notes* , 54 (2022).
- [49] L. Fidkowski, J. Haah, and M. B. Hastings, How Dynamical Quantum Memories Forget, *Quantum* **5**, 382 (2021).
- [50] G. Piccitto, A. Russomanno, and D. Rossini, Entanglement transitions in the quantum Ising chain: A comparison between different unravelings of the same Lindbladian, *Phys. Rev. B* **105**, 064305 (2022).
- [51] M. Fava, L. Piroli, T. Swann, D. Bernard, and A. Nahum, Nonlinear Sigma Models for Monitored Dynamics of Free

- Fermions, *Phys. Rev. X* **13**, 041045 (2023).
- [52] V. Ravindranath and X. Chen, Robust Oscillations and Edge Modes in Nonunitary Floquet Systems, *Phys. Rev. Lett.* **130**, 230402 (2023).
- [53] See Supplemental Material for details of the Gaussian-state simulation and additional numerical data.
- [54] A. Zabalo, M. J. Gullans, J. H. Wilson, R. Vasseur, A. W. W. Ludwig, S. Gopalakrishnan, D. A. Huse, and J. H. Pixley, Operator Scaling Dimensions and Multifractality at Measurement-Induced Transitions, *Phys. Rev. Lett.* **128**, 050602 (2022).
- [55] K. Mochizuki and R. Hamazaki, Absorption to fluctuating bunching states in nonunitary boson dynamics, *Phys. Rev. Res.* **6**, 013004 (2024).
- [56] A. Kumar, K. Aziz, A. Chakraborty, A. W. W. Ludwig, S. Gopalakrishnan, J. H. Pixley, and R. Vasseur, Boundary transfer matrix spectrum of measurement-induced transitions, *Phys. Rev. B* **109**, 014303 (2024).
- [57] A. D. Luca, C. Liu, A. Nahum, and T. Zhou, Universality classes for purification in nonunitary quantum processes (2024), arXiv:2312.17744 [cond-mat.stat-mech].
- [58] K. Mochizuki and R. Hamazaki, Measurement-Induced Spectral Transition (2024), arXiv:2406.18234 [quant-ph].
- [59] V. B. Bulchandani, S. L. Sondhi, and J. T. Chalker, Random-Matrix Models of Monitored Quantum Circuits, *J. Stat. Phys.* **191**, 55 (2024).
- [60] Z. Xiao, T. Ohtsuki, and K. Kawabata, Universal Stochastic Equations of Monitored Quantum Dynamics (2024), arXiv:2408.16974 [cond-mat.stat-mech].
- [61] A. Crisanti, G. Paladin, and A. Vulpiani, *Products of Random Matrices in Statistical Physics*, Vol. 104 (Springer-Verlag, Berlin, 1993).
- [62] S. V. Ershov and A. B. Potapov, On the concept of stationary Lyapunov basis, *Physica D* **118**, 167 (1998).
- [63] F. Ginelli, H. Chaté, R. Livi, and A. Politi, Covariant Lyapunov vectors, *J. Phys. A* **46**, 254005 (2013).
- [64] A. Y. Kitaev, Unpaired Majorana fermions in quantum wires, *Physics-Uspekhi* **44**, 131 (2001).
- [65] G. B. Mbeng, A. Russomanno, and G. E. Santoro, The quantum Ising chain for beginners, *SciPost Phys. Lect. Notes* , 82 (2024).
- [66] C. W. J. Beenakker, Random-matrix theory of Majorana fermions and topological superconductors, *Rev. Mod. Phys.* **87**, 1037 (2015).
- [67] K. Kawabata, R. Kobayashi, N. Wu, and H. Katsura, Exact zero modes in twisted Kitaev chains, *Phys. Rev. B* **95**, 195140 (2017).
- [68] S. Sang, Y. Li, T. Zhou, X. Chen, T. H. Hsieh, and M. P. Fisher, Entanglement Negativity at Measurement-Induced Criticality, *PRX Quantum* **2**, 030313 (2021).
- [69] C.-M. Jian, B. Bauer, A. Keselman, and A. W. W. Ludwig, Criticality and entanglement in nonunitary quantum circuits and tensor networks of noninteracting fermions, *Phys. Rev. B* **106**, 134206 (2022).
- [70] H. Lóio, A. De Luca, J. De Nardis, and X. Turkeshi, Purification timescales in monitored fermions, *Phys. Rev. B* **108**, L020306 (2023).
- [71] J. Merritt and L. Fidkowski, Entanglement transitions with free fermions, *Phys. Rev. B* **107**, 064303 (2023).
- [72] Z. Xiao and K. Kawabata, Topology of Monitored Quantum Dynamics (2024), arXiv:2412.06133 [cond-mat.stat-mech].